Experimental Study of Electrically Compact Retrodirective Monopole Antenna Arrays

Journal:	*Transactions on Antennas and Propagation*
Manuscript ID	AP1608-1112
Proposed Manuscript Type:	Paper
Date Submitted by the Author:	01-Aug-2016
Complete List of Authors:	Malyuskin, Oleksandr; ECIT, Fusco, Vincent; Queens University of Belfast, Electrical Eng
Key Words :	Antenna arrays, Antenna array mutual coupling, Antenna gain, Antenna measurements, Antenna radiation patterns, Diffraction, Electrically small antennas, Electromagnetic scattering, Near fields, Phase conjugation

Experimental Study of Electrically Compact Retrodirective Monopole Antenna Arrays

Oleksandr Malyuskin, Vincent Fusco, *Fellow, IEEE*

***Abstract*— Auto-pointing and angular super-resolution properties of the radiation patterns generated by an electrically compact retrodirective monopole antenna array are demonstrated experimentally for the first time. The operation of electrically compact (element spacings less than one fifth of the radiation wavelength) retrodirective antenna arrays that were theoretically considered in our previous work are confirmed by measurement. Particularly it is shown that the Direction-of-Arrival (DoA) information carried by an incident electromagnetic wave can be encoded into the evanescent near field of an electrically small resonant antenna array with a spatial rate higher than the spatial oscillation rate of the incident field in free space. Retrodirective array antenna matching and the feasibility of a frequency-division full-duplex communication link based on the proposed antenna arrays are also discussed.**

***Index Terms*— Antenna array, angular diffraction limit, monopole antennas, directive antennas, electromagnetic coupling, near field, radiation pattern, wireless communications**

I. Introduction

Electrically small antennas and antenna arrays have been extensively studied for several decades due to their theoretical and practical importance [1]-[6]. As a result of their small electrical size, these antennas and antenna arrays find many applications, including wireless communications, electromagnetic (EM) sensors, small aperture radars, compact microwave and mm-wave imaging systems [1], [6], [7]. Several interesting designs of electrically small antennas have been proposed recently. These include folded antenna geometries [1], [2], [6], [8], metamaterials [9]-[11], dielectric resonator antennas [1], [12] and biologically inspired resonantly loaded antennas [13], [14].

The design of electrically small antenna arrays with relatively high gain and practically useful bandwidth [3] represents a more challenging task than designing a single electrically small antenna, since the known rules for standard, half-wavelength spaced antenna arrays cannot be routinely applied due to complex near field EM coupling mechanisms [1], [3], [15].

An efficient approach to superdirective array realization [3] is based on the selection of the electrically small resonant antenna elements supporting large radiating currents that enable high unidirectional directivity of the order of 7-9dB even for simple 2-element antenna arrangements. It has been shown in [3], [15] that the spacings between the array elements cannot be made arbitrarily small due to accompanying significant radiation resistance drop, consequent antenna feeding mismatch and eventual array efficiency reduction.

One of the essential properties of any antenna array is its ability to control the radiation pattern in receive and/or transmit mode. For antenna arrays used in wireless communications an omnidirectional radiation pattern is commonly employed in the receive mode to ensure complete spatial coverage for signal reception [16]. At the same time, a narrow beam pattern radiated towards the communicator by the antenna array would add significant benefits to a communication system, particularly increased signal-to-noise ratio at the receiver for the same input power, lower bit-error rate (BER) reduced EIRP and EM pollution.

One class of electrically compact antenna arrays with electronically reconfigurable radiation patterns has been proposed in [17]. This is based on a circular dipole or monopole antenna array topology with a central active element and a number of passive parasitic antennas with variable reactive loading [18], [19] (ESPAR antenna). ESPAR antennas allow electronic beam scanning with improved signal-to-noise ratio and reduced BER of the received signal however ESPAR beam scanning requires considerable digital processing with regard to inputs related to the DoA and channel/propagation characteristics [18],[19].

In our previous companion paper [15] we proposed a fundamentally new class of electrically compact antenna terminals with omnidirectional radiation pattern in receive mode and auto-pointing superdirective radiation pattern in transmit mode, with auto-pointing requiring dedicated electronic circuitry performing EM signal phase conjugation, [20]-[22]. The EM phenomena enabling electrically compact retrodirective antenna array (RDA) operation are theoretically considered in full detail in [15]. Particularly, it has been demonstrated that the DoA information carried by an incident EM wave can be encoded into the array excitation vector in the receive mode with a spatial rate higher than the incident field spatial oscillation rate in free space. This can be understood by expanding the scattered field in the array environment into its plane wave spectrum where evanescent harmonics with fast spatial oscillation rate contribute dominantly into the Fresnel and quasistatic near field, [15], [23], [24]. This leads to much larger "effective" aperture of the dense array exceeding its geometrical area [25]. Next, phase conjugation of the receive excitation vector (amplitudes and phases of voltages across the antenna array terminals) and

Manuscript received xx. 2016. The work is supported under the EPRSC grant EP/N020391/1 and the Leverhulme Trust UK research grant RPG-2013-117.
The authors are with The Institute of Electronics, Communications and Information Technology, Queen's University Belfast, Belfast, BT3 9DT, U.K. (e-mail: o.malyuskin@qub.ac.uk; v.fusco@ee.qub.ac.uk).

their re-application across the respective antenna terminals in transmit (retrodirective) mode leads to angular super-resolution spatial far-field patterns with auto-pointing properties. Angular super-resolution [26] arises as a result of the "effective" aperture of the array being larger than its physical size which in-turn requires high intensity of the evanescent field in the array environment that exceeds the magnitude of the incident field. This is possible when the antenna elements operate in EM resonance leading to high electric currents that generate large scattered field.

In this paper we experimentally study the EM performance of a 4-element retrodirective top-loaded resonance monopole array of compact electrical size ~λ/4, and inter-element-spacings λ/6, λ is the radiation wavelength. The retrodirection patterns measured in the azimuthal plane and the auto-pointing and angular super-resolution properties of these electrically compact RDA are demonstrated for the first time.

II. Antenna Array Geometry and Measurement Setup

A. RDA Geometry

A 4-element top-loaded monopole RDA, Fig. 1, is illuminated in the azimuthal plane by a vertically-polarized EM plane wave with monochromatic, exp(-*iωt*), frequency carrier. A full-wave FEKO [28] simulation model was used to predict monopole RDA performance.

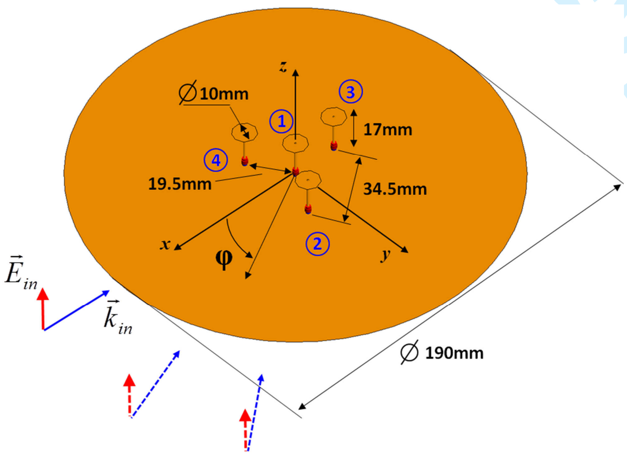

(a)


(b)

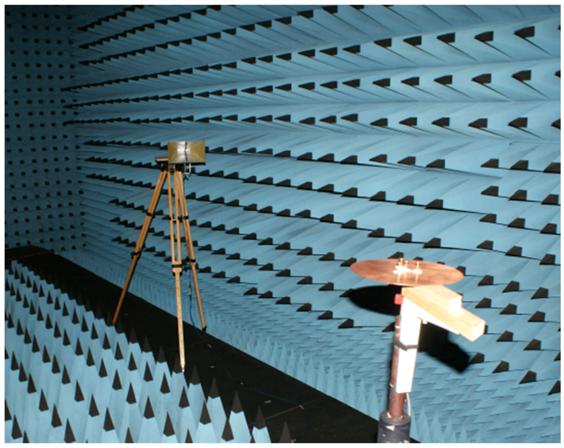
(c)

Fig.1. (a) Antenna geometry and FEKO simulation model; (b) fabricated prototype; (c) measurement setup in anechoic chamber. The distance between the horn antenna and RDA is 3.5m. In a) the antenna ports are labelled by the numbers in blue circles. In b) the monopole antennas are fed via 50Ω SMA coaxial connectors with flanges attached to the circular ground plane by plastic bolts. The ground plane is mounted on a bracket and attached to a wooden turntable, c).

B. Measurement Setup for the RDA in Receive Mode

The measurement setup schematic diagram for the RDA in receive (RX) mode is shown in Fig. 2.

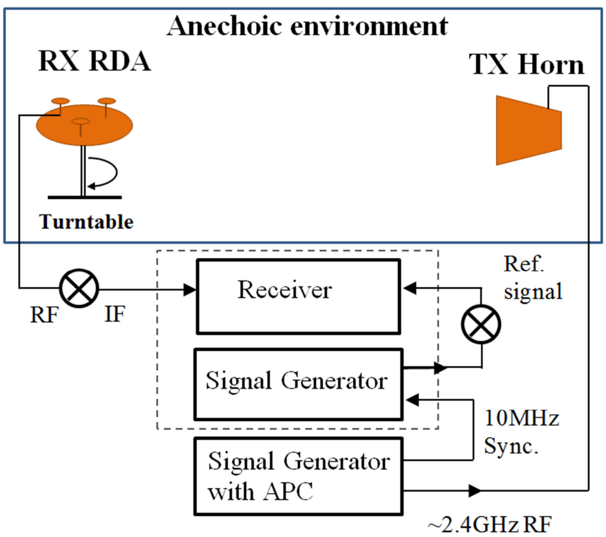

Fig.2. Measurement setup diagram for the compact RDA in receive mode.

In this arrangement the monopole RDA is illuminated by a transmitting (TX) vertically polarized horn antenna in the anechoic environment. The horn antenna is fed by a continuous wave signal at ~2.4GHz generated by a signal generator Agilent E8257D with both amplitude and phase control (APC). This generator is synchronized at 10MHz with a signal generator/frequency synthesizer Hewlett Packard 8341B which forms a part of standard far-field anechoic chamber equipment (in dashed rectangle). The signal is received by each RDA port sequentially in the 360 degree range for the fixed TX horn position. The RX signal is down converted to ~1GHz and processed by the 1780 Scientific Atlanta amplitude and phase receiver thus RX amplitudes and phases across each RDA port are recorded for DoA in the 360 degree range.

C. Measurement Setup for the RDA in Retrodirective Mode

In the RDA TX (retrodirective) mode the array excitation vector is formed using the amplitudes for the specific DoA and conjugated phases recorded at each array element, corresponding to this DoA. Phase conjugation can be realized by the analog or digital circuitry operators [22]. In this paper we generate the array excitation vector using a signal generator with amplitude and phase control since this allows us to measure the antenna array gain independent of particular phase conjugation circuitry realization. The excitation vector is applied to each port sequentially and the final far field radiation pattern obtained by linear superposition of the partial RX voltages at the horn antenna. The measurement setup diagram for the RDA TX mode is shown in Fig.3.

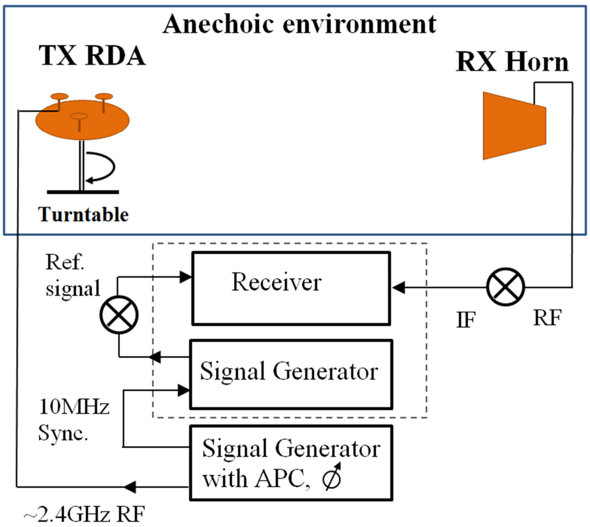

Fig.3. Measurement setup diagram for the RDA in TX/retrodirective mode.

III. Experimental Results

A. RDA Antenna Return Loss

First we discuss RDA antenna matching. The monopole RDA in Fig. 1 has been designed to explore the effect of mutual near field coupling on the antennae feed port matching. It can be seen, Fig.1a), b) that there are three outer elements 2,3,4 that are exposed in a scattering field with magnitude smaller than the scattering field magnitude acting on central element 1. It is well known [1], [3], [15] that larger reactive coupling between antennas (or, equivalently, near scattering field exposure) leads to lower radiation resistance and poorer antenna matching with respect to a 50Ω feeding port. This fact is illustrated by Fig. 4a) where the measured (using Agilent PNA network analyzer 8361C) and simulated return loss $|S_{nn}|$ is presented for antenna ports n=1,2,3,4 with reference port impedance 50Ω. It can be seen that in the frequency band around 2.4-2.7GHz matching is acceptable for outer antenna elements and is very poor for the central antenna element which prevents its practical use.

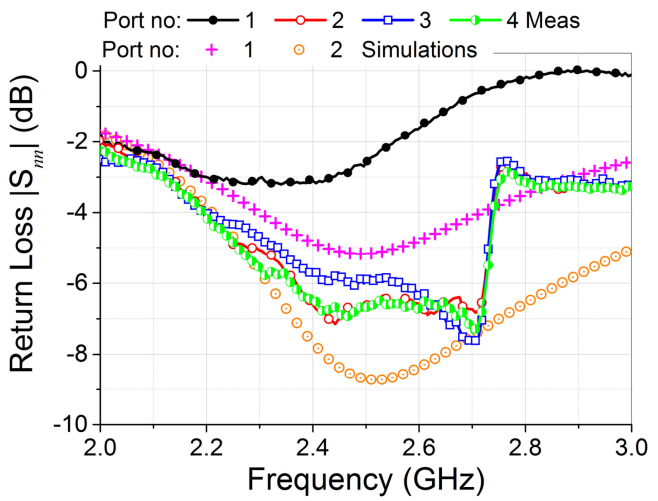

(a)

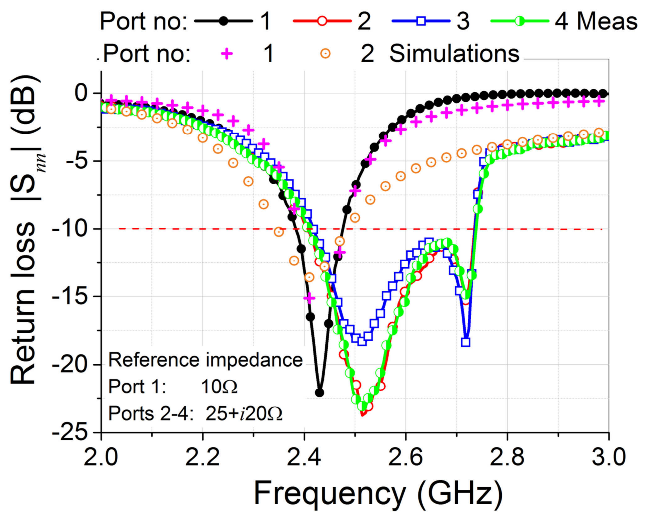

(b)

Fig.4. Simulated and measured return loss, $|S_{nn}|$ for the RDA antenna ports n=1,2,3,4. (a) Reference port impedance 50Ω (b) Reference port impedance 10Ω for port 1, impedance 25+i20Ω for ports 2,3,4 (measurements) and reference port impedance 25Ω for ports 2,3,4 (simulations). Simulation data are the same for ports 2,3,4 and therefore only data for port 2 are shown.

Consequently, a series of measurements has been performed to find out the optimal reference port impedance, Fig.4b). It can be seen that when the outer elements are fed through the ports with reference impedance 25+i20Ω the antenna are well-matched at -10dB in the ~13% fractional bandwidth (2.4-2.73GHz). At the same time the central element is matched only in 4% fractional bandwidth (2.39-2.48GHz). Also, the reference impedance for the central element is quite low, 10Ω, and therefore matching for this element can suffer from losses within the antenna system. It should be noted that for the considered type of monopole RDA phase conjugated circuits can be printed on the back side of the ground plane and the required reference impedance can be obtained using lumped components, therefore 50Ω feeding is not a prerequisite.

B.RDA in Receive Mode

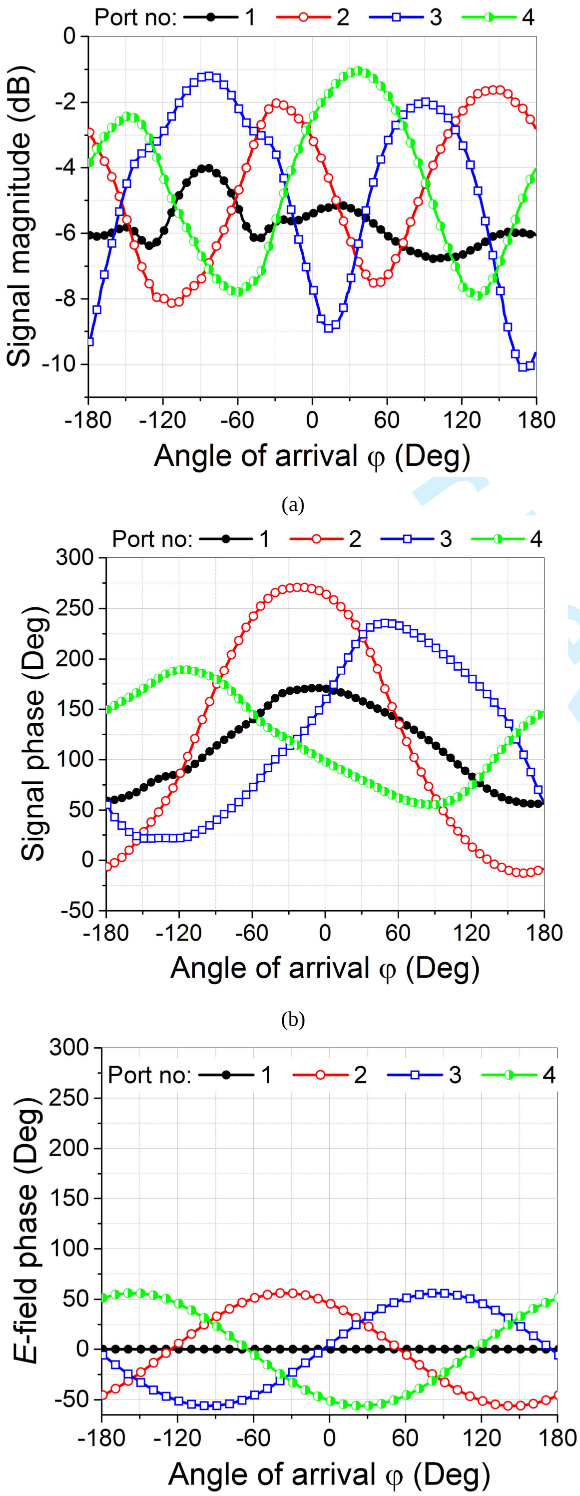

(a)

(b)

(c)

Fig.5.Measured RX signal magnitude (a) and phase (b) across the monopole RDA ports at 2.42GHz. Simulated phase of the incident plane wave at the positions corresponding to monopole arm centers (with antenna elements removed).

Fig. 5 shows the measured received signal magnitude, Fig.5a) and phase, Fig.5b) across the RDA antenna ports at 2.42GHz. Fig.5c) depicts the simulated phase of the incident plane wave in the positions corresponding to the monopole arm centers with the antennae removed. Graphs b), c) are plotted in the same scale for comparison. It can be seen that the RDA RX signal phases (and phase shifts between the ports) experience much larger variation (more than 100 degrees) with respect to the angle of arrivals than the respective phase of the incident field, [15]. This can be explained [15] by the generation of large scattered field, $\vec{E}_{sc}(\vec{r})$ with magnitude exceeding that of the magnitude of the incident field in the dense antenna array environment. From [15],[29] the plane wave representation of the scattered field is

$$\vec{E}_{sc}(\vec{r}) \sim \sum_{n=1}^{N}\Phi_n \int_{-\infty}^{\infty} \vec{\mathrm{E}}_{sc}(\vec{k})\exp[i\vec{\chi}\cdot(\vec{\rho}-\vec{\rho}_n)]\exp(\pm i k_z z)\,d\vec{\chi} \quad (1)$$

where $\vec{r}=\vec{\rho}+z\vec{z}_0$ is the observation point radius vector, $\vec{\chi}$ is a spectral parameter (partial wavevector), $\vec{\rho}_n$ is the *n*-th antenna position in the azimuthal plane, $k_z^2+|\vec{\chi}|^2=k_0^2$, $k_0=2\pi/\lambda$ is a free space wavenumber, and spectral amplitudes $\vec{\mathrm{E}}_{sc}(\vec{k})$ are given in [15].

In the near field the dominant role is played by the evanescent harmonics with wavenumbers $|\chi|>k_0$, $\chi=|\vec{\chi}|$, these are larger than the free space wave number k_0. These evanescent harmonics oscillate in the array plane with the spatial oscillation rate ~ $2\pi/\chi$ higher than the oscillation rate of the incident field (given by the wavelength λ) in free space. Therefore the DoA phase carried by the factor $\Phi_n=\exp(i\vec{k}_{in}\cdot\vec{\rho}_n)$, $\vec{k}_{in}$ the incident wavevector is encoded into these evanescent components with higher spatial oscillation rate than is possible with the propagating waves in free-space. This phenomenon manifests itself in significant phase shifts, ~ χd , d is the antenna element spacings, between the received signal phases across the RDA antenna ports, Fig. 5b) as compared to the incident field phase variation in free space, Fig.5c). It should also be noted that another consequence of the resonance scattered field $\vec{E}_{sc}(\vec{r}) >> \vec{E}_{in}(\vec{r})$ generated within the antenna array environment leads to the "effective" aperture [25] of the RDA being substantially larger than its geometric area resulting in angular super-resolution of its radiation patterns [15].

B.RDA in Transmit Mode

In the retrodirective mode the phase-conjugated array excitation vector on receive is re-applied to the respective RDA antenna terminals. Since only one signal generator was available for the amplitude and phase control, the RDA ports were excited sequentially, and the resulting far-field spatial patterns obtained using linear superposition of the signals corresponding to each of the individual port excitations. In order to calculate relative gain a reference dipole was used, so that gain was calculated as a ratio of the signal power received by the horn antenna from the RDA array to the power received by the horn from a reference dipole, for the same input power. Since the standard definition of gain does not include antenna mismatch loss [3], the return loss was taken at -15dB, for 50Ω feeding. The "realized" gain including mismatch losses is smaller by approximately 30%. It should be noted that for the reference port impedance matching as in Fig.4b) the "realized" gain is the same as the relative gain presented in Fig.6. The retrodirective radiation patterns were measured at 2.42 GHz in the DoA range 0-120^o with 30^o step, the results are shown in Fig.6. Full-wave FEKO simulations are also presented for comparison.

Figs.6a)-d) show that the radiation pattern angular bandwidth $\Delta\theta_{-3dB}$ at -3dB level is around 90 degrees regardless the DoA angle. The resolution-limited radiating aperture [25] corresponding to the RDA size L ~λ/4 would generate a pattern with beamwidth $\Delta\theta_{-3dB} \approx \lambda/L$ (Rad) of 4 radians (229 degrees).

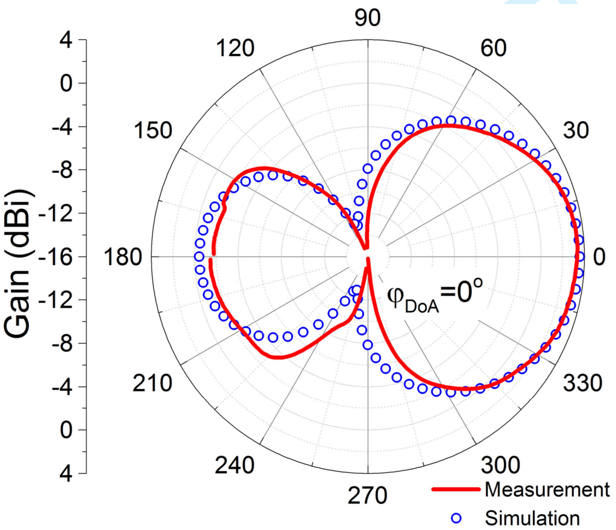

(a)

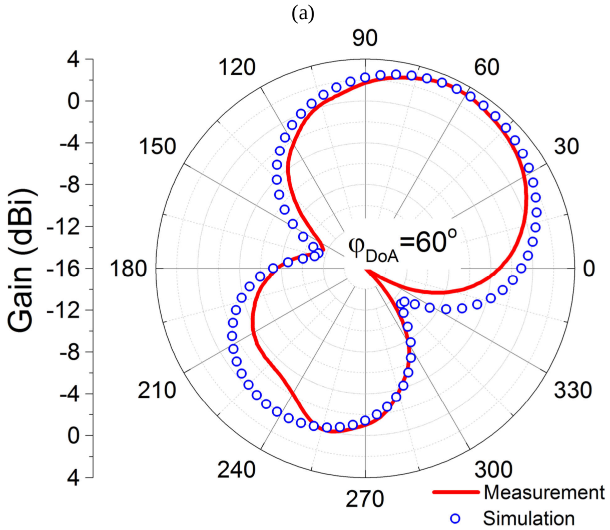

(b)

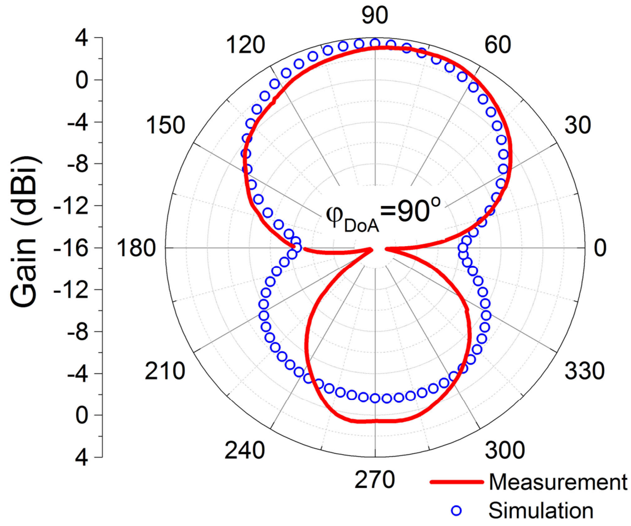

(c)

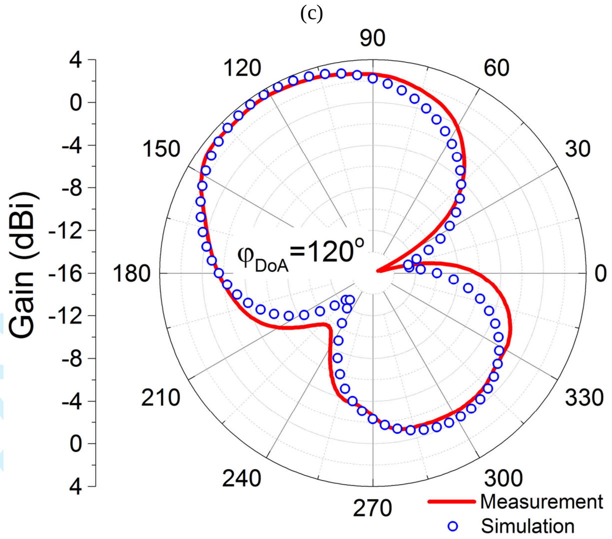

(d)

Fig.6.Measured (solid lines) and simulated (hollow dots) radiation patterns for DoA 0, 60, 90 and 120 degrees.

C. Frequency-division full-duplex communication link feasibility

Let us consider now the feasibility of a frequency-division full-duplex communication link based on the electrically compact RDAs. In this scenario the communicator sends a downlink signal towards the RDA at the carrier frequency f_1 and receives the uplink signal at the carrier frequency f_2. From the practical point of view [22] it is interesting to establish if the retrodirective properties of the RDA are preserved if the array excitation vector obtained at the frequency f_1 is applied to generate the retrodirected signal at carrier frequency f_2. The measurement results carried out for DoA 0 degrees are shown in Fig.7. It can be seen that when the carrier frequency deviates within 1% the retrodirective properties of the compact monopole RDA are fairly well preserved. However, carrier frequency deviation of more than 1% leads, in general, to significant retrodirective pattern pointing error. Therefore if a frequency-division full-duplex link is required, a carrier signal at downlink frequency f_1 has to be accompanied with a pilot signal at the uplink frequency f_2 to generate an uplink array excitation vector.

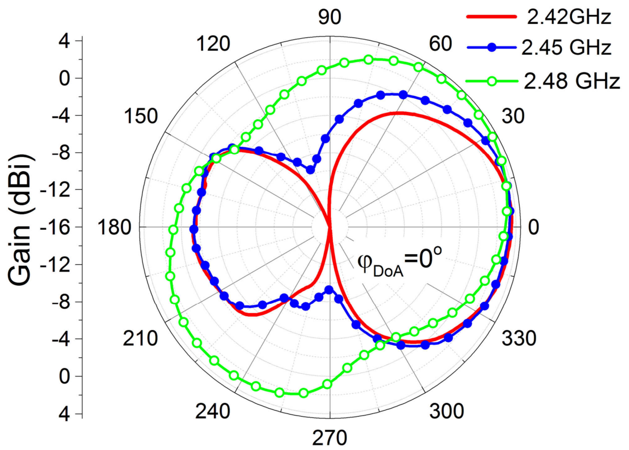

Fig.7.Measured retrodirective radiation patterns for the situation when the monopole RDA excitation vector at 2.42GHz is used to generate the retrodirective radiation patterns at close frequencies 2.45GHz and 2.48GHz.

IV. Conclusions

Angular super-resolution and auto-pointing properties of the radiation patterns generated by an electrically compact retrodirective monopole antenna array were shown experimentally. Particularly it was demonstrated that the angular beamwidth at -3dB of a four-element array with a quarter-wavelength characteristic spatial size is 90 degrees for an arbitrary DoA. In contrast, the resolution-limited angular bandwidth of the quarter-wavelength aperture radiation pattern is around 230 degrees. Thus arrays of the proposed type enable physical super-resolution based on DoA information encoding into the highly oscillatory evanescent harmonics generated within the antenna array environment.

It should be noted that this mechanism of super-resolution presented in this paper is essentially different from the classical super-resolution phenomenon based on the super-oscillatory behavior of the antenna element currents and fields [30]-[32]. This in turn means that the proposed antenna arrays are free from the drawbacks pertinent to the classical super-oscillatory arrays [33], namely extremely narrow frequency bandwidth of operation, high sensitivity to geometrical tolerances, etc.

Moreover it has been shown that for antenna elements with $\lambda/6$ spacings, a 13% fractional bandwidth of return loss at -10dB level can be readily achieved by tuning the reference impedance within practical limits.

A very attractive feature of the proposed compact arrays in their ability to retrodirect the signal automatically without any digital signal processing or DoA estimation. No compensation of antenna coupling effects is also required.

It is believed that the proposed antenna terminals could find applications in energy-efficient wireless communications, and EM systems where space is a premium.

Acknowledgement

The authors are thankful to Mr. Kieran Rainey for fabrication of the monopole RDA prototype and assistance with the measurements.

References

[1] R.C. Hansen, R. E. Collin, Small Antenna Handbook, John Wiley & Sons, Inc. 2011.
[2] K. Fujimoto, A. Henderson, K. Hirasawa, and J. R. James, Small Antennas, Wiley, 1987.
[3] A. D. Yaghjian, T. H. O'Donnell, E. E. Altshuler, and S. R. Best, "Electrically small supergain end-fire arrays", *Radio Science*, vol. 43, RS3002, pp1-13, 2008.
[4] Altshuler, E. E., T. H. O'Donnell, A. D. Yaghjian, and S. R. Best, "A monopole superdirective array", *IEEE Trans. Antennas Propag*., vol. 53, no. 8, pp. 2653–2661, Aug. 2005.
[5] R.W.P. King, "Supergain Antennas and the Yagi and circular arrays", *IEEE Trans Antennas Propagat*., vol.37, no.2, pp. 178-186, Feb.1989.
[6] M. J. Slater, C.D. Schmitz, M.D. Anderson, et al., "Demonstration of an Electrically Small Antenna Array for UHF Direction-of-Arrival Estimation", *IEEE Trans Antennas Propagat*., vol.61, no.3, pp. 1371-1377, Mar 2013.
[7] H.-T. Liu, S. Gao, and T.-H. Loh, "Electrically Small and Low Cost Smart Antenna for Wireless Communication", *IEEE Trans. Antennas Propagat*., vol.60, no.3, pp. 1540-1549, March 2012.
[8] S. Best, "The performance properties of electrically small resonant multiple-arm folded wire antennas", *IEEE Antennas Propag. Mag*., vol. 47, pp. 13–27, 2005.
[9] R. W. Ziolkowski, P. Jin, and C.-C. Lin, "Metamaterial-Inspired Engineering of Antennas", *Proc. IEEE*, vol. 99, pp. 1720-1731, 2011.
[10] A. D. Yaghjian, "Increasing the supergain of electrically small antennas using metamaterials," *Proc. 3rd Eur. Conf. Antennas Propag*. (*EuCAP'09*), 2009, pp. 858–860.
[11] K. Buell, H. Mosallaei and K. Sarabandi, "Metamaterial Insulator Enabled Superdirective Array", *IEEE Trans. Antennas Propagat*., vol. 55, no.4, pp. 1074-1085, 2007.
[12] Y.-M. Pan, K. W. Leung, and Kai Lu," Compact Quasi-Isotropic Dielectric Resonator Antenna With Small Ground Plane", *IEEE Trans. Antennas Propagat*., vol.62, no.2, pp. 577-585, Feb. 2014.
[13] N. Behdad, M.A. Al-Joumayly and M. Li, "Biologically Inspired Electrically Small Antenna Arrays With Enhanced Directional Sensitivity", *IEEE Trans. Antennas Propagat. Letters*, vol.10, pp. 361-364, 2011.
[14] N. Behdad, M.A. Al-Joumayly and M. Li, "Biologically-Inspired Antenna Arrays Based on the Hearing Mechanism of the Parasitoid Fly Ormia Ochracea", *IEEE Int. Symp. Antennas . Propagat.* (*APSURSI 2011*), pp. 1526-1529, 2011.
[15] O. Malyuskin, V. Fusco, "Ultracompact Retrodirective Antenna Arrays With Superdirective Radiation Patterns", *IEEE Trans. Antennas Propagat*., vol.64, no.7, pp. 2923 - 2935, July 2016.
[16] S. Saunders, A. Aragón-Zavala, Antennas and Propagation for Wireless Communication Systems, Wiley 2007.
[17] C. Sun, A. Hirata, T. Ohira, N. Karmakar, "Fast Beamforming of Electronically Steerable Parasitic Array Radiator Antennas: Theory and Experiment", *IEEE Trans. Antennas Propagat*., vol.57, no.7, pp. 1819-1832, July 2004.
[18] H.-T. Liu, S. Gao, and T.-H. Loh, "Compact MIMO Antenna With Frequency Reconfigurability and Adaptive Radiation Patterns", *IEEE Trans. Antennas Propagat. Lett.*, vol. 12, pp. 269-272, 2013.
[19] Y. Zhou, R. S. Adve, Sean Victor Hum, "Design and Evaluation of Pattern Reconfigurable Antennas for MIMO Applications", *IEEE Trans. Antennas Propagat*., vol.62, no.3, pp. 1084-1092, March 2014.
[20] V. Fusco, O. Malyuskin, N. Buchanan, "Active phase conjugating lens with sub-wavelength resolution capability", *IEEE Trans. Antennas Propagat*., vol.58, no.3, pp. 798-808, 2010.
[21] O. Malyuskin, V. Fusco, A. Schuchinsky, "Microwave phase conjugation using nonlinearly loaded wire arrays", *IEEE Trans. Antennas Propagat*., vol.54, no.1, pp. 192-203, 2006.
[22] V. Fusco, N. Buchanan, "Developments in retrodirective array technology", *IET Microw. Antennas Propagat*., vol. 7, no. 2, pp. 131–140, 2013.

[23] T.B. Hansen, A.D. Yaghjian, Plane-Wave Theory of Time-Domain Fields : Near-Field Scanning Applications, Wiley IEEE, 1999.

[24] O. Malyuskin, V. Fusco, "Near field focusing using phase conjugating impedance loaded wire lens", *IEEE Trans. Antennas Propagat.*, vol. 58, no.9, pp. 2884-2893, 2010.

[25] E.V. Jull, Aperture Antennas and Diffraction Theory, Peter Peregrinus, 1981.

[26] R.C. Hansen, "Fundamental limitations in antennas", *Proceedings IEEE*, vol. 69, no.2, pp. 170-182, Feb. 1981.

[27] H.A. Wheeler, "The radian sphere around a small antenna", *Proc. IRE*, vol. 47, pp. 1325-1331, 1959.

[28] Electromagnetic solver FEKO, www.feko.info

[29] T.B. Hansen, A.D. Yaghjian, Plane-Wave Theory of Time-Domain Fields : Near-Field Scanning Applications, Wiley IEEE, 1999.

[30] S.A. Schelkunoff, "A Mathematical Theory of Linear Arrays", *Bell Syst. Tech. Journal*, vol. 22, pp. 80-107, 1943.

[31] A. M. H. Wong and G. V. Eleftheriades, "Superoscillations without Sidebands: Power-Efficient Sub-Diffraction Imaging with Propagating Waves", *Scientific Reports* vol. 5, article no: 8449, pp.1-6, 2015. doi:10.1038/srep08449

[32] E.T.F. Rogers, J. Lindberg, T. Roy, et al, "A super-oscillatory lens optical microscope for subwavelength imaging", *Nature Materials Lett*. Vol.11, pp. 432-435, May 2012.

[33] N. Yaru, "A note on super-gain antenna arrays," *Proc. IRE*, vol 39, pp. 1081–1085, Sep. 1951.

Experimental Study of Electrically Compact Retrodirective Monopole Antenna Arrays

What is the problem being addressed by the manuscript and why is it important to the Antennas & Propagation community? (limited to 100 words).

The design, fabrication and experimental characterization of electrically compact (with spacings less than one fifth of the radiation wavelength) retrodirective antenna arrays with auto-pointing and super-resolution radiation patterns. These antenna terminals could offer significant benefits to energy-efficient wireless communication systems, wireless imaging modalities and radars with reduced aperture/footprint size.

* What is the novelty of your work over the existing work? (limited to 100 words).

Auto-pointing and angular super-resolution properties of the radiation patterns generated by an electrically compact retrodirective monopole antenna array are demonstrated experimentally for the first time. Particularly, it is demonstrated that the Direction-of-Arrival (DoA) information carried by an incident electromagnetic wave can be encoded into the evanescent near field of an electrically small resonant antenna array with a spatial rate higher than the spatial oscillation rate of the incident field in free space.

* Provide up to three references, published or under review, (journal papers, conference papers, technical reports, etc.) done by the authors/coauthors that are closest to the present work. Upload them as supporting documents if they are under review or not available in the public domain. Enter “N.A.” if it is not applicable.

O. Malyuskin, V. Fusco, “Ultracompact Retrodirective Antenna Arrays With Superdirective Radiation Patterns”, IEEE Trans. Antennas Propagat., vol.64, no.7, pp. 2923 - 2935, July 2016.

V. Fusco, N. Buchanan, “Developments in retrodirective array technology”, IET Microw. Antennas Propagat., vol. 7, no. 2, pp. 131–140, 2013.

* Provide up to three references (journal papers, conference papers, technical reports, etc.) done by other authors that are most important to the present work. Enter “N.A.” if it is not applicable.

A. D. Yaghjian, T. H. O’Donnell, E. E. Altshuler, and S. R. Best, “Electrically small supergain end-fire arrays”, Radio Science, vol. 43, RS3002, pp1-13, 2008.

H.-T. Liu, S. Gao, and T.-H. Loh, “Electrically Small and Low Cost Smart Antenna for Wireless Communication”, IEEE Trans. Antennas Propagat., vol.60, no.3, pp. 1540-1549, March 2012.

Y. Zhou, R. S. Adve, Sean Victor Hum, “Design and Evaluation of Pattern Reconfigurable Antennas for MIMO Applications”, IEEE Trans. Antennas Propagat., vol.62, no.3, pp. 1084-1092, March 2014.